Achieving stable fiber coupling of quantum dot telecom C-band single-photons to an SOI photonic device ⊘

Stephanie Bauer ✉ ⓘ ; Dongze Wang; Niklas Hoppe ⓘ ; Cornelius Nawrath ⓘ ; Julius Fischer ⓘ ;
Norbert Witz; Mathias Kaschel; Christian Schweikert ⓘ ; Michael Jetter ⓘ ; Simone L. Portalupi ⓘ ;
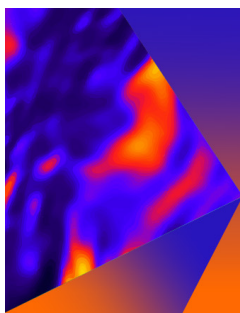Manfred Berroth; Peter Michler ⓘ

Check for updates

View Online   Export Citation   CrossMark

23 February 2024 10:34:44

Achieving stable fiber coupling of quantum dot telecom C-band single-photons to an SOI photonic device

View Online   Export Citation   CrossMark

Stephanie Bauer,[1,a)] (iD) Dongze Wang,[1] Niklas Hoppe,[2] (iD) Cornelius Nawrath,[1] (iD) Julius Fischer,[1] (iD) Norbert Witz,[1,b)]
Mathias Kaschel,[3] Christian Schweikert,[2] (iD) Michael Jetter,[1] (iD) Simone L. Portalupi,[1] (iD)
Manfred Berroth,[2] and Peter Michler[1] (iD)

AFFILIATIONS

[1]Institut für Halbleiteroptik und Funktionelle Grenzflächen, Center for Integrated Quantum Science and Technologie (IQST)
and SCoPE, University of Stuttgart, 70569 Stuttgart, Germany
[2]Institute of Electrical and Optical Communications Engineering, University of Stuttgart, 70569 Stuttgart, Germany
[3]Institut für Mikroelektronik Stuttgart (IMS CHIPS), 70569 Stuttgart, Germany

a)Author to whom correspondence should be addressed: Stephanie.Bauer@ihfg.uni-stuttgart.de
b)Current address: Twenty-One Semiconductors, Kiefernweg 4, 72654 Neckartenzlingen, Germany.

ABSTRACT

The well-established silicon-on-insulator platform is very promising for large-scale integrated photonic and quantum photonic technologies due to the mature manufacturing technology and integration density. Here, we present an efficient and stable fiber-to-chip coupling, which enables the injection of single photons from telecom quantum dots into a silicon-on-insulator photonic chip. Two additional fibers further couple the chip to single-photon detectors. The approach chosen to achieve steady fiber-chip coupling is based on the use of grating couplers steadily packaged with angled single-mode fibers. Using this technique, coupling efficiencies between the fiber and the SOI chip as high as 69.1% per grating coupler (including the taper losses) are reached. The effective interface between the quantum light generated by quantum dots and the silicon components is verified via the measurement of the second-order correlation function using a Hanbury–Brown and Twiss setup. With $g^{(2)}(0) = 0.051 \pm 0.001$, it clearly proves the single-photon nature of the injected QD photons. This demonstrates the reliability of the interfacing method and opens the route to employ telecom quantum dots as non-classical light sources with high complexity silicon photonic functionalities.

Several research and technology fields, like quantum information processing and quantum communication, would strongly benefit from the realization of on-chip quantum photonics. The implementation of large-scale integrated quantum photonic technologies requires on-chip reconfigurable waveguide (WG) circuits as well as single-photon sources and detectors.[1] Much progress has been made in recent years in demonstrating complex quantum circuits in many material platforms, such as lithium niobate,[2,3] silica,[4] silicon nitride,[5] gallium arsenide,[3,6,7] indium phosphide,[8] and silicon.[9] Among all these platforms, the silicon-on-insulator (SOI) platform is highly attractive as it is well developed for classical photonic applications. It, therefore, deploys a high component density, mature fabrication techniques and compatibility with the telecom regime, and the complementary metal–oxide–semiconductor (CMOS) technology. Quantum key distribution,[10]

linear optical quantum computation,[9,11] and boson sampling[12] on a chip were demonstrated recently. However, the lack of on-demand non-classical light sources, directly incorporated into silicon chips, has spurred research activities in the field of nonlinear processes to generate non-classical light states. The probabilistic nature of the emission process poses a challenge in the maximally achievable experimental complexity and efficiency. The use of on-demand quantum light sources would have a strong impact on the achievable scalability. In addition, a highly pure single-photon emission will play a key role in the implementation of computation protocols otherwise limited by multiphoton events. Semiconductor quantum dots (QDs) are seen as one of the most promising sources of quantum light, since they can generate on demand light.[13–15] As silicon photonics are highly optimized to operate with light in the telecom C-band (1530 to 1565 nm), the use of

23 February 2024 10:34:44

semiconductor QDs emitting in this wavelength range would be beneficial. For semiconductor QDs, the InAs/InP[16–19] and InAs/InGaAs/GaAs[20–22] material systems proved the capability of reaching this wavelength. The latter are based on the versatile and well-developed GaAs material platform QDs,[23] which normally emit at near-infrared wavelengths, but the wavelength is shifted to higher wavelengths through the employment of a metamorphic buffer design.[20] Until now, the interface of semiconductor QDs emitting in the telecom C-band and Si photonics has been a challenging task. There are different approaches to integrate QDs into silicon photonics. In addition to the development of QDs based on Si/Ge heterostructures,[24] a hybrid approach was recently used to integrate QDs on a silicon chip, emitting at wavelengths around 1310 nm[25] and 1160 nm.[26] However, until now, no coupling between an SOI chip and a QD emitting in the telecom C-band has been realized. Furthermore, semiconductor QDs require cryogenic temperatures, making the design of the silicon chip more challenging. Therefore, alternative approaches are based on funneling light on the silicon chip from external sources. These have the advantage that light sources and silicon chip can be freely designed, and the latter can even kept at room temperature. For this scope, high in-coupling efficiency needs to be achieved, ideally with a mechanically stable connection that does not require realignment. Grating couplers[27,28] have the advantages of high alignment tolerances and can be fabricated on every position on the chip. Moreover, they have recently been demonstrated to reach coupling efficiencies of up to 89% (-0.5 dB)[29] in the telecom C-band.

In this paper, we present an efficient, stable, and scalable fiber-to-chip coupling, based on grating couplers, which enables the injection of single photons from InGaAs/GaAs QDs, emitting in the telecom C-band into an SOI photonic chip.

An artistic illustration of the overall device can be seen in Fig. 1(a).

The fundamental part is an SOI chip, which is fabricated on the 250 nm SOI platform. On the chip, a waveguide circuit is implemented, which includes a 50:50 multi-mode interference splitter (MMI). The input and output ports of the MMI are fed by single-mode waveguides. These waveguides are then tapered to the width of input and output grating couplers. Here, the used grating couplers are similar to the grating couplers presented by Hoppe et al.,[29] where record coupling efficiencies with losses as low as -0.5 dB (89% coupling efficiency) were reached. While for the design presented by Hoppe et al.,[29] the filling factor and grating period were used for the apodization; here only the filling factor has been varied. The design for grating couplers used here reaches coupling losses of minimal -0.76 dB (83.9%, without taper losses).

In order to achieve this value, back-etched aluminum backside reflectors are employed to reflect the light, which leaks into the substrate, in the upward direction. Additionally, through a careful choice of the trench width and period for each grating groove, the overlap integral between the radiated field profile of the grating coupler and the Gaussian fiber mode is maximized. The design of the used grating coupler with varying grating groove widths can be seen in a scanning electron microscope (SEM) image in Fig. 1(c). Trenches reaching grating groove widths down to 60 nm were realized using e-beam lithography.

In this paper, the approach chosen to achieve stable fiber-chip coupling is based on the use of these aforementioned grating couplers
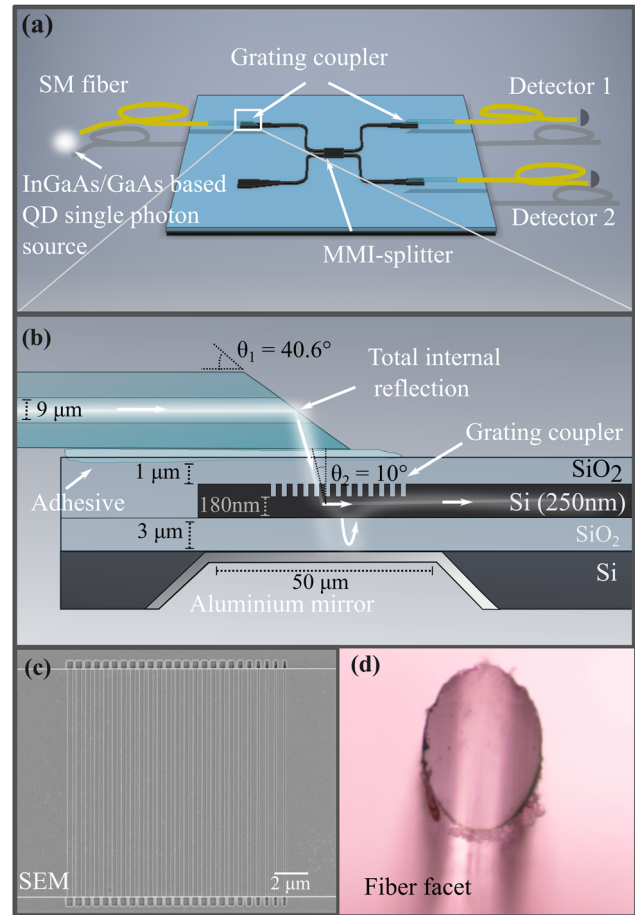

FIG. 1. (a) Schematic of the experimental setup. (b) Schematic side view showing the coupling principle with an angled single-mode fiber. (c) SEM picture of the used grating coupler with varying grating groove width. (d) Polished fiber facet.

together with angle-polished single-mode fibers [see Figs. 1(b) and 1(d)]. This fabrication and alignment procedure allows us to adjust multiple fibers, whereby each can be positioned individually relative to its optimal position over the grating coupler. By polishing the fiber tips at a precise angle, they can be steadily glued horizontally to the chip, while the incident light, reflected via total internal reflection, matches the acceptance angle of the grating couplers [see Fig. 1(b)]. Thereby, the parallel arrangement to the chip surface allows the adhesive to have a maximum contact area, which enables the mechanically stable bonding. For this scope, first, the jacket of standard SMF-28 fibers is removed before the fiber coating is stripped off by a hot jacket stripper (HJS-02). Afterward, the fiber is cleaved to produce a 90 facet angle using a commercial high precision cleaver CT-30 from Fujikura. Then, the fibers are clamped into an aluminum holder, enabling the grinding of the fiber under a specific angle, which is predefined by the aluminum holder itself. To reach the acceptance angle, the fiber is polished under a facet angle of $\theta_1 = 40.6°$ using different polishing sheets. For the stable gluing process, it is necessary to align the fibers along the waveguide axis and parallel to the chip surface. Moreover,
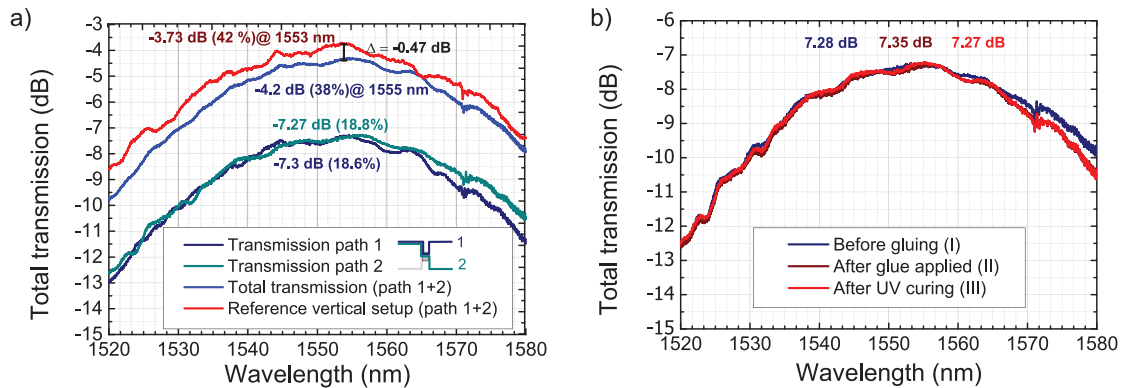
FIG. 2. (a) Transmission for the upper and the lower path of the chip and the overall transmission for both arms together. This transmission is compared to the near-vertical measurement of the same structure on the chip. (b) Transmission through the chip before and after gluing and after UV curing.

the rotation along the fiber axis is adjusted. Afterward, index matching Norland optical adhesive is applied near the fiber. Due to capillary effects, the adhesive gets sucked into the space between the fiber and the waveguides covering the whole fiber length. Special attention needs to be given that not too much adhesive is applied to avoid covering the fiber tip. This would spoil the total internal reflection condition. Afterward, the total transmission through the system is maximized by optimizing the x-, y-, and z-positions of the fibers relative to the grating couplers using movable three-dimensional piezo positioning stages. In the final position, the adhesive is cured using UV-light exposure. Afterward, the fiber-cladding-free parts of the fibers are glued additionally to a customized holder, which is mounted under the chip. This second gluing step prevents the glued fiber tips from any mechanical stress and unwanted cleaving and, thus, enables mechanical stability during measurement and transportation.

Using this packaging procedure, one input and two output fibers are steadily glued to the chip. To evaluate the performance of the device, the total transmission of the chip is the direct experimentally measured parameter. First step of evaluation is the measurement of the same MMI-WG structure on the chip in the near-vertical configuration before the actual gluing procedure on exactly the same structure is performed. For the near-vertical configuration, the in- and outcoupling is achieved via standard cleaved fibers with their axes aligned to an angle of $\theta_2 = 10°$ to the vertical, reaching a total transmission of -3.73 dB for both channels together [see Fig. 2(a)]. After gluing three fibers to the chip, the total losses are -7.27 dB (equivalent to a total transmission of 18.8%) for the lower channel and -7.3 dB (equivalent to a total transmission of 18.6%) for the upper channel. Combining the transmission through both paths results in a total transmission of -4.2 dB (equivalent to a total transmission of 38.0%).

Comparing the total transmission to the in advance measured transmission of the same chip in near vertical alignment, only -0.47 dB additional losses are caused by the presented packaging method. Moreover, the wavelength maxima for both channels are centered at the same wavelengths between 1550 and 1555 nm. The contribution of the adhesive is negligible as the losses of the packaging using the adhesive are only -0.07 dB lower compared to the configuration, where two angled fibers but no glue are used [see Fig. 2(b)].

Furthermore, the curing of the adhesive has led to no further reduction of the coupling efficiency.

The total loss includes also the chip-related internal losses, being independent from the gluing method. These are the grating coupler losses, the waveguide losses, the bending losses of the 90 bends, and the MMI losses. They are estimated, measuring (in near vertical alignment) equally designed structures on different chips and are listed in Table I. The waveguide losses for this fabrication procedure can be estimated to be -4.5 dB/cm leading to -0.55 dB per path, whereas for the four 90 bends, they are estimated as -0.08 dB and for the MMI -0.4 dB. Together, this results in a loss of -1.03 dB per path.

To calculate the actual reached coupling efficiency of one grating coupler in our packaged system, we subtract these chip internal losses (WG losses, bending losses, and MMI losses) from our measured total transmission. This yields the coupling loss of one grating coupler of -1.54 dB (equivalent to a coupling efficiency of 69.6%, including the taper losses) for one grating coupler and the adjacent taper. To compare the horizontal gluing method to the vertical unstable alignment method, we measured the coupling losses for one grating coupler and the adjacent taper section for a near vertical alignment to be -1.3 dB (equivalent to a coupling efficiency of 74.1%, including the taper losses). This means that the coupling losses of our packaged system are only -0.24 dB (4.5% lower coupling efficiency) higher than the coupling losses of a vertical unstable alignment.

Having achieved a highly efficient and mechanically stable fiber-chip coupling, the effective interface between the quantum light generated by a QD and the silicon components is verified via the use as a beam splitter for a Hanbury-Brown and Twiss measurement of the second-order auto-correlation function.

TABLE I. The contribution of the implemented elements on the SOI chip to the overall losses.

	Waveguide losses	MMI losses	90° bending losses
Loss/element	-4.5 dB/cm	-0.4 dB/MMI	0.02 dB/bend
Amount	1.225 cm	1 MMI	4 bends
Total losses	-0.55 dB	-0.4 dB	-0.08 dB

The single-photon source used here consists of a planar sample structure with InAs QDs on an InGaAs metamorphic buffer layer on top of 23 pairs of AlAs/GaAs functioning as a distributed Bragg reflector. The QDs are capped by 220 nm InGaAs. Apart from the thinner (220 nm), non-linearly graded metamorphic buffer layer and a thinner cap layer, the structure is based on the design of the sample described in Ref. 20. The QD is kept in a helium-flow cryostat at 4 K and is excited using continuous-wave above-bandgap excitation emitting single photons in the telecom C-band. The corresponding spectrum can be seen in the inset of Fig. 3 with an emission wavelength of 1564 nm at 4 K for the QD transition in question (highlighted in red). The emitted light is spectrally filtered to select the bright, narrow transition (see inset of Fig. 3) and then coupled into a single-mode fiber. Through the fiber packaging, the single photons are reliably injected into a second chip with comparable performances and a peak efficiency around 1560 nm and split into two paths by the on-chip integrated silicon MMI beam splitter. Via the two stable packaged output fibers, the single photons can then be directed to the superconducting nanowire single-photon detectors. Fig. 3 shows the measured second-order auto correlation function. The data were fitted accounting for bunching behavior at finite delay times. A clear photon anti-bunching is visible for zero time delay with $g^{(2)}(0) = 0.0512 \pm 0.001$, given by the fit. This is comparable to a reference second-order correlation function, measured with an off-chip fiber beam splitter, where the fit is yielding a $g^{(2)}(0) = 0.0370 \pm 0.001$. The small deviation between these values is attributed to the background coincidences. However, the preservation of single-photon behavior within the packaged fiber SOI chip system is clearly demonstrated as the value is comparable to the fiber beam splitter.

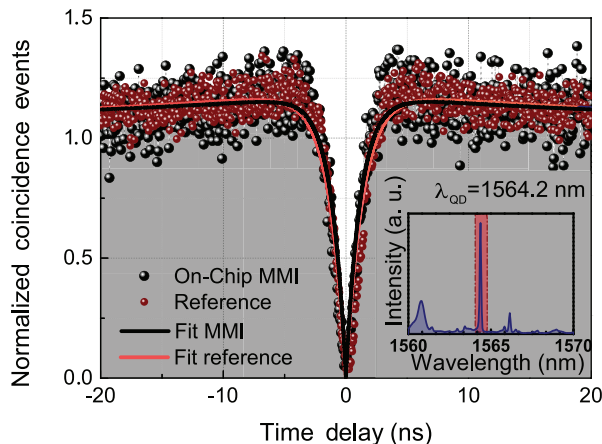This work demonstrates that the developed approach can be employed to realize a stable and efficient fiber-to-chip coupling. This enabled for the first time the injection of telecom C-band QDs into an SOI-photonic chip. The low insertion losses and the robust design make this technique suitable for the use with non-classical light states, where low losses and long integration time are needed for exploiting complex quantum photonics. The capability of independently interface multiple fibers makes this approach highly flexible and ready to be used with any chip design employing grating couplers. The use with fiber-arrays, where multiple fibers are mounted in an array, would enable the up scaling to an approach with many fibers on the same chip. Moreover, even lower insertion losses are possible: By improvement of the fiber polishing, the additional losses compared to the vertical measurement could be minimized to nearly zero, as the gluing procedure showed nearly no further losses. With the employment of the grating coupler design presented in Hoppe et al.,[29] coupling losses as low as −0.5 dB are expected to be reached. Moreover, by optimization of the fabrication parameters, the coupling losses could come closer to the theoretical value of −0.33 dB[27] (which corresponds to a coupling efficiency of 94%).

AUTHOR DECLARATIONS

Conflict of Interest

The authors have no conflicts of interest to declare.

DATA AVAILABILITY

The data that support the findings of this study are available from the corresponding author upon reasonable request.

FIG. 3. Second order correlation measurement with the packaged system and with an off-chip fiber beam splitter as reference on the same QD transition and the same excitation conditions. The inset shows the spectra of the chosen QD. The combined, raw count rates on the SNSPDs (Single Quantum, detection efficiency 80% at 1550 nm) are found to be 120 kcps and 20 kcps for the reference and on-chip measurement, respectively. The difference is due to the overall efficiency of the on-chip device (19.15%) and losses due to additional fiber absorption and fiber connections that are necessary for the on-chip measurement as the device is placed in a different lab than the source and detectors.

REFERENCES

[1]S. Hepp, M. Jetter, S. L. Portalupi, and P. Michler, "Semiconductor quantum dots for integrated quantum photonics," Adv. Quantum Technol. **2**, 1970053 (2019).

[2]A. Boes, B. Corcoran, L. Chang, J. Bowers, and A. Mitchell, "Status and potential of lithium niobate on insulator (lnoi) for photonic integrated circuits," Laser Photonics Rev. **12**, 1700256 (2018).

[3]C. Wang, M. Zhang, M. Yu, R. Zhu, H. Hu, and M. Loncar, "Monolithic lithium niobate photonic circuits for Kerr frequency comb generation and modulation," Nat. Commun. **10**, 978 (2019).

[4]A. Politi, M. J. Cryan, J. G. Rarity, S. Yu, and J. L. O'Brien, "Silica-on-silicon waveguide quantum circuits," Science **320**, 646–649 (2008).

[5]A. Rahim, E. Ryckeboer, A. Z. Subramanian, S. Clemmen, B. Kuyken, A. Dhakal, A. Raza, A. Hermans, M. Muneeb, S. Dhoore et al., "Expanding the silicon photonics portfolio with silicon nitride photonic integrated circuits," J. Lightwave Technol. **35**, 639–649 (2017).

[6]M. Schwartz, E. Schmidt, U. Rengstl, F. Hornung, S. Hepp, S. L. Portalupi, K. Llin, M. Jetter, M. Siegel, and P. Michler, "Fully on-chip single-photon Hanbury–Brown and Twiss experiment on a monolithic semiconductor–superconductor platform," Nano Lett. **18**, 6892–6897 (2018).

[7]M. Pooley, D. Ellis, R. Patel, A. Bennett, K. Chan, I. Farrer, D. Ritchie, and A. Shields, "Controlled-NOT gate operating with single photons," Appl. Phys. Lett. **100**, 211103 (2012).

[8]B. J. Isaac, B. Song, S. Pinna, L. A. Coldren, and J. Klamkin, "Indium phosphide photonic integrated circuit transceiver for fmcw lidar," IEEE J. Sel. Top. Quantum Electron. **25**, 1–7 (2019).

[9]X. Qiang, X. Zhou et al., "Large-scale silicon quantum photonics implementing arbitrary two-qubit processing," Nat. Photonics **12**, 534–539 (2018).

[10] V. Scarani, H. Bechmann-Pasquinucci, N. J. Cerf, M. Dušek, N. Lütkenhaus, and M. Peev, "The security of practical quantum key distribution," Rev. Mod. Phys. **81**, 1301 (2009).

[11] J. L. O'Brien, "Optical quantum computing," Science **318**, 1567–1570 (2007).

[12] S. Paesani, Y. Ding, R. Santagati, L. Chakhmakhchyan, C. Vigliar, K. Rottwitt, L. K. Oxenløwe, J. Wang, M. G. Thompson, and A. Laing, "Generation and sampling of quantum states of light in a silicon chip," Nat. Phys. **15**, 925–929 (2019).

[13] L. Schweickert, K. D. Jöns, K. D. Zeuner, S. F. Covre da Silva, H. Huang, T. Lettner, M. Reindl, J. Zichi, R. Trotta, A. Rastelli et al., "On-demand generation of background-free single photons from a solid-state source," Appl. Phys. Lett. **112**, 093106 (2018).

[14] L. Hanschke, K. A. Fischer, S. Appel, D. Lukin, J. Wierzbowski, S. Sun, R. Trivedi, J. Vučković, J. J. Finley, and K. Müller, "Quantum dot single-photon sources with ultra-low multi-photon probability," npj Quantum Inf. **4**, 43 (2018).

[15] N. Somaschi, V. Giesz, L. De Santis, J. Loredo, M. P. Almeida, G. Hornecker, S. L. Portalupi, T. Grange, C. Anton, J. Demory et al., "Near-optimal single-photon sources in the solid state," Nat. Photonics **10**, 340–345 (2016).

[16] T. Miyazawa, K. Takemoto, Y. Sakuma, S. Hirose, T. Usuki, N. Yokoyama, M. Takatsu, and Y. Arakawa, "Single-photon generation in the 1.55-μm optical-fiber band from an inas/inp quantum dot," Jpn. J. Appl. Phys. **44**, L620 (2005).

[17] M. Benyoucef, M. Yacob, J. Reithmaier, J. Kettler, and P. Michler, "Telecom-wavelength (1.5 μm) single-photon emission from inp-based quantum dots," Appl. Phys. Lett. **103**, 162101 (2013).

[18] T. Müller, J. Skiba-Szymanska, A. Krysa, J. Huwer, M. Felle, M. Anderson, R. Stevenson, J. Heffernan, D. A. Ritchie, and A. Shields, "A quantum light-emitting diode for the standard telecom window around 1,550 nm," Nat. Commun. **9**, 862 (2018).

[19] M. Anderson, T. Müller, J. Huwer, J. Skiba-Szymanska, A. Krysa, R. Stevenson, J. Heffernan, D. Ritchie, and A. Shields, "Quantum teleportation using highly coherent emission from telecom c-band quantum dots," npj Quantum Inf. **6**, 14 (2020).

[20] M. Paul, F. Olbrich, J. Höschele, S. Schreier, J. Kettler, S. L. Portalupi, M. Jetter, and P. Michler, "Single-photon emission 1.5 μm from MOVPE-grown InAs quantum dots on InGaAs/GaAs metamorphic buffers," Appl. Phys. Lett. **111**, 033102 (2017).

[21] C. Nawrath, H. Vural, J. Fischer, R. Schaber, S. Portalupi, M. Jetter, and P. Michler, "Resonance fluorescence of single in (Ga) As quantum dots emitting in the telecom c-band," Appl. Phys. Lett. **118**, 244002 (2021).

[22] K. D. Zeuner, K. D. Jöns, L. Schweickert, C. Reuterskiöld Hedlund, C. Nunez Lobato, T. Lettner, K. Wang, S. Gyger, E. Schöll, S. Steinhauer et al., "On-demand generation of entangled photon pairs in the telecom c-band with InAs quantum dots," ACS Photonics **8**, 2337 (2021).,

[23] Single Quantum Dots - Fundamentals, Applications and New Concepts, edited by P. Michler (Springer-Verlag, Berlin/Heidelberg/New York, 2003).

[24] F. Boscherini, G. Capellini, L. Di Gaspare, F. Rosei, N. Motta, and S. Mobilio, "Ge-Si intermixing in Ge quantum dots on Si(001) and Si," Appl. Phys. Lett. **76**(111), 682–684 (2000).

[25] J.-H. Kim, S. Aghaeimeibodi, C. J. Richardson, R. P. Leavitt, D. Englund, and E. Waks, "Hybrid integration of solid-state quantum emitters on a silicon photonic chip," Nano Lett. **17**, 7394–7400 (2017).

[26] R. Katsumi, Y. Ota, A. Osada, T. Yamaguchi, T. Tajiri, M. Kakuda, S. Iwamoto, H. Akiyama, and Y. Arakawa, "Quantum-dot single-photon source on a cmos silicon photonic chip integrated using transfer printing," APL Photonics **4**, 036105 (2019).

[27] W. S. Zaoui, A. Kunze, W. Vogel, M. Berroth, J. Butschke, F. Letzkus, and J. Burghartz, "Bridging the gap between optical fibers and silicon photonic integrated circuits," Opt. Express **22**, 1277–1286 (2014).

[28] Y. Ding, C. Peucheret, H. Ou, and K. Yvind, "Fully etched apodized grating coupler on the soi platform with −0.58 dB coupling efficiency," Opt. Lett. **39**, 5348–5350 (2014).

[29] N. Hoppe, W. S. Zaoui, L. Rathgeber, Y. Wang, R. H. Klenk, W. Vogel, M. Kaschel, S. L. Portalupi, J. Burghartz, and M. Berroth, "Ultra-efficient silicon-on-insulator grating couplers with backside metal mirrors," IEEE J. Sel. Top. Quantum Electron. **26**, 1–6 (2020).

23 February 2024 10:34:44